PIP2 and talin join forces to activate integrin

Adam Orłowski,[a,#] Sampo Kukkurainen,[b,#] Annika Pöyry,[a] Sami Rissanen,[a] Ilpo Vattulainen,[a,c] Vesa P. Hytönen,[b] and Tomasz Róg[a,*]

[a] Department of Physics, Tampere University of Technology,
P. O. Box 692, FI-33101 Tampere, Finland

[b] BioMediTech, University of Tampere, FI-33520 Tampere, Finland, and
Fimlab Laboratories Ltd., FI-33520 Tampere, Finland

[c] Department of Physics and Chemistry,
MEMPHYS—Center for Biomembrane Physics, University of Southern Denmark,
Campusvej 55, DK-5230 Odense M, Denmark

[*] To whom correspondence should be addressed: Tomasz Róg, Department of Physics, Tampere University of Technology, Korkeakoulunkatu 10, FI-33101 Tampere, Finland; E-mail: tomasz.rog@tut.fi
[#] The two leading authors contributed equally to this work.

ABSTRACT
Integrins are major players in cell adhesion and migration, and malfunctions in controlling their activity are associated with various diseases. Nevertheless, the details of integrin activation are not completely understood, and the role of lipids in the process is largely unknown. Herein, we show using atomistic molecular dynamics simulations that the interplay of phosphatidylinositol 4,5-bisphosphate (PIP2) and talin may directly alter the conformation of integrin αIIbβ3. Our results provide a new perspective on the role of PIP2 in integrin activation and indicate that the charged PIP2 lipid headgroup can perturbate a clasp at the cytoplasmic face of the integrin heterodimer.

Keywords: Lipid-protein interaction, membrane protein, lipid, phosphatidylinositol, molecular dynamics simulation, computer simulation

---

1. Introduction

Multicellular organisms provide well-defined and tightly controlled mechanisms for cell-cell and cell-extracellular matrix interactions. The group of receptors called integrins plays a central role in these mechanisms. Integrins and integrin-mediated processes are essential for normal cell functions such as signaling, cell migration, adhesion to the local extracellular environment, and leukocyte function. Moreover, integrins play a role in cancer progression and metastasis, and certain tumor types have been found to exhibit higher levels of specific integrins. This makes the integrin-associated signal complex an important spot for cancer therapy development.[1]

Integrins are heterodimeric transmembrane receptors that in mammals are composed of 18 different α and 8 β subunits.[2,3] These proteins respond to both extracellular (outside-in) and intracellular (inside-out) stimuli, connect the extracellular matrix to the cytoskeleton, and pass signals across the plasma membrane in both directions.[3] This requires a properly controlled integrin activation mechanism that involves conformational changes within the integrin heterodimer. In the case of the inside-out signaling, the changes eventually lead to an extended integrin conformation with a high affinity for extracellular ligands.[2,4] Proper control of integrin activation and thus cellular communication with the external environment is crucial for many physiologically relevant processes. Perturbation of this equilibrium can lead to constitutive activation of the integrin[5] and result in bleeding disorders.[3,6,7,8]

Talin, a 2541-residue long cytoplasmic protein,[9,10,11] is one of the triggers that binds to integrin and activates it (inside-out) in the first stages of cell attachment.[12,13] Importantly, the conformational changes induced by talin in the transmembrane part of the integrin αβ complex are crucial for the inside-out activation process.[14] More specifically, the N-terminal FERM domain of talin binds to the NPxY motif of the integrin β tail, induces a reorganization of the integrin heterodimer, and contributes to integrin activation.[11,15,16,17,18] Attachment of talin to a membrane is enhanced by a lipid known as phosphatidylinositol 4,5-bisphosphate (PIP2),[19,20] which can enforce talin to undergo conformational changes that expose the integrin β-tail binding site in its head domain.[11,21,22,23]

The role of PIP2 in integrin activation is intriguing given that PIP2 is a major phosphoinositide of the inner plasma membrane.[24,25] Moreover, talin itself binds and activates phosphatidylinositol phosphate kinase type Iγ[26,27] and may thereby regulate the local concentration of PIP2 in the membrane. PIP2 is able to regulate many important cellular processes including vesicular trafficking, platelet activation, and organization of the cytoskeleton,[28,29,30] and it may control several steps in focal adhesion.[19,20,31] PIP2 can also affect protein conformation,[32,33,34,35] target cytoplasmic proteins to the membrane, and stabilize protein oligomers.[31,36]

In this article, we focus on clarifying the importance of lipid membrane composition in the conformational modulation of integrins. In particular, we focus on the role of PIP2 in the complex integrin activation process. Despite very well documented earlier studies that showed the role of talin-PIP2 interactions in the integrin activation,[19,22] and the fact that single lipid species have recently been found to regulate the conformation and function of several membrane proteins,[37,38,39] it is striking that the effects of direct integrin-

PIP2 interactions have not received attention until now.

Here, by using extensive atomistic molecular dynamics (MD) simulations, we show that PIP2 can interfere with the integrin heterodimer and therefore have implications for the integrin activation process. We discuss the possible joint action of PIP2 with talin, and define regions in all talin head subdomains F0-F3 that are able to interact with phosphatidylcholine and PIP2 lipids in the studied membranes. Altogether, our results give new insight into integrin-talin interactions with an emphasis on PIP2 and its role in integrin activation.

2. Materials and Methods

2.1 Molecular modeling of the integrin-talin complex

Short and long versions of the mouse talin-1 head domain were prepared using Modeller versions 9.9 and 9.10, respectively.[40] The crystal structure of talin-1 subdomains F2-F3 in a complex with β3-integrin (PDB ID: 1MK7)[15] was used as a template for the short talins containing the residues 209-400. Missing residues were added to the talin-1 head domain structure (PDB ID: 3IVF)[41] using the NMR structure of the talin head subdomains F0-F1 (PDB ID: 2KMA)[42] to yield a talin-1 head domain with the residues 2-398 (Δ139-168). Talin-integrin contacts were modeled using two talin-integrin structures (PDB IDs: 1MK7[15] and 3G9W).[43] The transmembrane domains of the integrin αβ dimer and the free β3 tail were modeled using NMR structures of the αIIbβ3 integrin as templates (PDB IDs: 2K9J,[44] 2KNC,[45] and 2KV9[46]).

2.2 Atomistic molecular dynamics simulations

Extensive atomistic molecular dynamics simulations were performed for the integrin αIIbβ3 and the integrin-talin complex together with a lipid bilayer comprised of either pure 1,2-dioleoyl-sn-glycero-3-phosphocholine (DOPC) or a 9:1 molar mixture of DOPC and phosphatidylinositol-4,5-bisphosphate (PIP2) (Figure S1; see Supplementary Information (SI)). We simulated systems of the integrin heterodimer consisting of transmembrane and cytoplasmic domains of αIIbβ3 in a complex with talin. Talin was present in two different configurations (either with the talin head domain (F0-F3) or with a fragment of talin head (F2-F3)), and for the purpose of having controls, systems consisting of the integrin heterodimer without talin were also studied. All these configurations, except for integrin without talin, were simulated in both membrane compositions. Some of the simulations were repeated for improved sampling. This resulted in a total of eight simulated systems (Table 1), each of which was simulated for 500 or 750 nanoseconds, altogether generating 4.5 microseconds of simulation results. The simulations were performed at a physiological salt concentration of 150 mM KCl. Counter ions were included to neutralize the total charge of the system. To control that the simulations are long enough, we calculated the mean square displacement of the center of mass of lipid molecules in the membrane plane (Figure S2; SI). The data obtained indicate that during the simulation time lipids diffuse on average 4-5 nm, which is 5-6 times the diameter of the lipids in the membrane plane.

Table 1
Composition of the simulated systems. F0-F3 and F2-F3 correspond to the talin domains included in the systems. The abbreviation PIP refers to systems with PIP2 (and DOPC) lipids, while NO-PIP refers to systems

without PIP2 lipids. The subscripts A and B stand for two independent runs of the same system. The control systems with PIP2 but without talin are represented by $PIP_{CONTROL}$.

System	Integrin	Talin (F0-F3)	Talin (F2-F3)	DOPC	PIP2	Water	K^+	Cl^-	Simulation time (μs)
PIP_{F0-F3}	1	1	-	844	96	113310	703	319	0.5
PIP_{F2F3-A}	1	-	1	440	50	60559	365	169	0.5
PIP_{F2F3-B}	1	-	1	440	50	60559	365	169	0.5
$NO\text{-}PIP_{F0-F3}$	1	1	-	950	0	114470	320	320	0.5
$NO\text{-}PIP_{F2F3-A}$	1	-	1	439	0	56631	158	162	0.5
$NO\text{-}PIP_{F2F3-B}$	1	-	1	439	0	56631	158	162	0.5
$PIP_{CONTROL-A}$	1	-	-	420	50	56182	358	155	0.75
$PIP_{CONTROL-B}$	1	-	-	420	50	56182	358	155	0.75

The OPLS all-atom force field was used to describe the interactions for all molecules except for lipids.[47] For lipids, a compatible lipid-refined version of the OPLS all-atom force field was applied.[48] For water, the TIP3P model that is compatible with the OPLS parameterization was employed.[49] The system setup used in this study is identical to that employed in previous simulations of lipid bilayers with the OPLS all-atom parameterization by the authors.[50,51] Periodic boundary conditions with the minimum image convention were employed in all three dimensions. The length of each hydrogen atom covalent bond was preserved by the LINCS algorithm.[52] The integration time step was set to 2 fs and the simulations were carried out at constant pressure (1 bar) and temperature (310 K). The temperature and pressure were controlled by the v-rescale and Parrinello–Rahman methods, respectively.[53,54] The temperatures of the solute and solvent were coupled separately. For pressure, a semi-isotropic scaling was employed. The Lennard-Jones interactions were cut off at 1.0 nm. For electrostatic interactions, the particle mesh Ewald method was employed with a real space cut-off of 1.0 nm, B-spline interpolation (6^{th} order), and a direct sum tolerance of 10^{-6}.[55] The simulations were performed with the GROMACS 4.5.5 simulation package.[56]

3. Results and discussion

3.1 PIP2 acting on the integrin dimer can break the Arg995-Asp723 salt bridge

The transmembrane domain of integrin possesses two interaction interfaces that stabilize the inactive conformation of the dimer.[14] One is formed between the highly conserved (GFFKR) motif of αIIb integrin and the hydrophobic residues Trp715 and Ile719 of β3 integrin within the membrane core, stabilized by a cytoplasmic salt bridge between Arg995 in αIIb and Asp723 in β3 integrin. These interactions are referred to as the inner membrane clasp (IMC). Further away from the cytoplasm, the interaction of the β3 residue Gly708 with the αIIb G972xxxG976 motif establishes the outer membrane clasp (OMC). Importantly, mutations of residues in either of these interaction sites (IMC and OMC) result in perturbed interactions of the transmembrane (TM) helices that can lead to a constantly active integrin.[14,44] In this respect, our particular interest is the salt bridge Arg995-Asp723 of the IMC.

By using atomistic molecular dynamics simulations, we investigated the interactions between PIP2

and the talin-integrin complex. The number of hydrogen bonds between PIP2 and each of the protein domains in the complex (integrin αIIb, β3, and talin) are shown in Table 2. A more detailed overview of the interactions between the integrin complex residues and PIP2 lipids is shown in Figure 1, Table S1 and Table S2, where the number of contacts between the atoms of integrin αIIb and β3 and atoms of PIP2 during the last 300 ns of the simulations are reported. Two residues were defined as being in contact when two heavy atoms of different molecules were located at a distance of 0.35 nm or less. Some residues in both αIIb and β3 integrin show a very high affinity towards PIP2. This applies to residues that are already outside the transmembrane helix in the water phase, such as Lys994, Arg995, and Arg997 in integrin αIIb, and His722, Arg724, Lys725, Lys729, and Arg736 in integrin β3. Interestingly, both from visual inspection (see Figure 2), and from the analyses of the number of hydrogen bonds between the residue Arg995 and PIP2 in time (Table 2), one can conclude that the PIP2 headgroup can find its way to the positively charged residue Arg995 and establish a bond with it through negatively charged phosphate groups. This interaction led to the breakage of the Arg995-Asp723 salt bridge (Figure 2B-C, Figure 3), and it took place spontaneously after less than 300 ns of the simulation time in two out of three simulations, where PIP2 was present. It has been shown that this salt bridge is crucial for the stability of the integrin αIIbβ3 dimer, and once it is broken, integrin activation can take place.[2,5,57] The local concentration of PIP2 might thus translate to integrin activation.

Table 2
Average number of hydrogen bonds between integrin, talin, or the αIIb residue Arg995, and PIP2 lipids. The data were calculated over the last 300 ns of the simulation time, regardless of the total simulation length. Errors are 0.2 or less. A hydrogen bond was judged to be formed when the acceptor-donor distance is ≤ 0.325 nm and the angle between the acceptor–donor vector and the covalent bond donor–hydrogen is ≤ 35°.[58]

System	Integrin αIIb – PIP2	Integrin β3 – PIP2	Talin – PIP2	Arg995 – PIP2
$PIP_{F0\text{-}F3}$	3.50	6.28	25.30	1.68
$PIP_{F2F3\text{-}A}$	3.17	4.66	17.67	3.00
$PIP_{F2F3\text{-}B}$	2.85	4.53	17.46	0
$PIP_{CONTROL\text{-}A}$	8.68	8.10	—	0
$PIP_{CONTROL\text{-}B}$	11.99	4.66	—	0

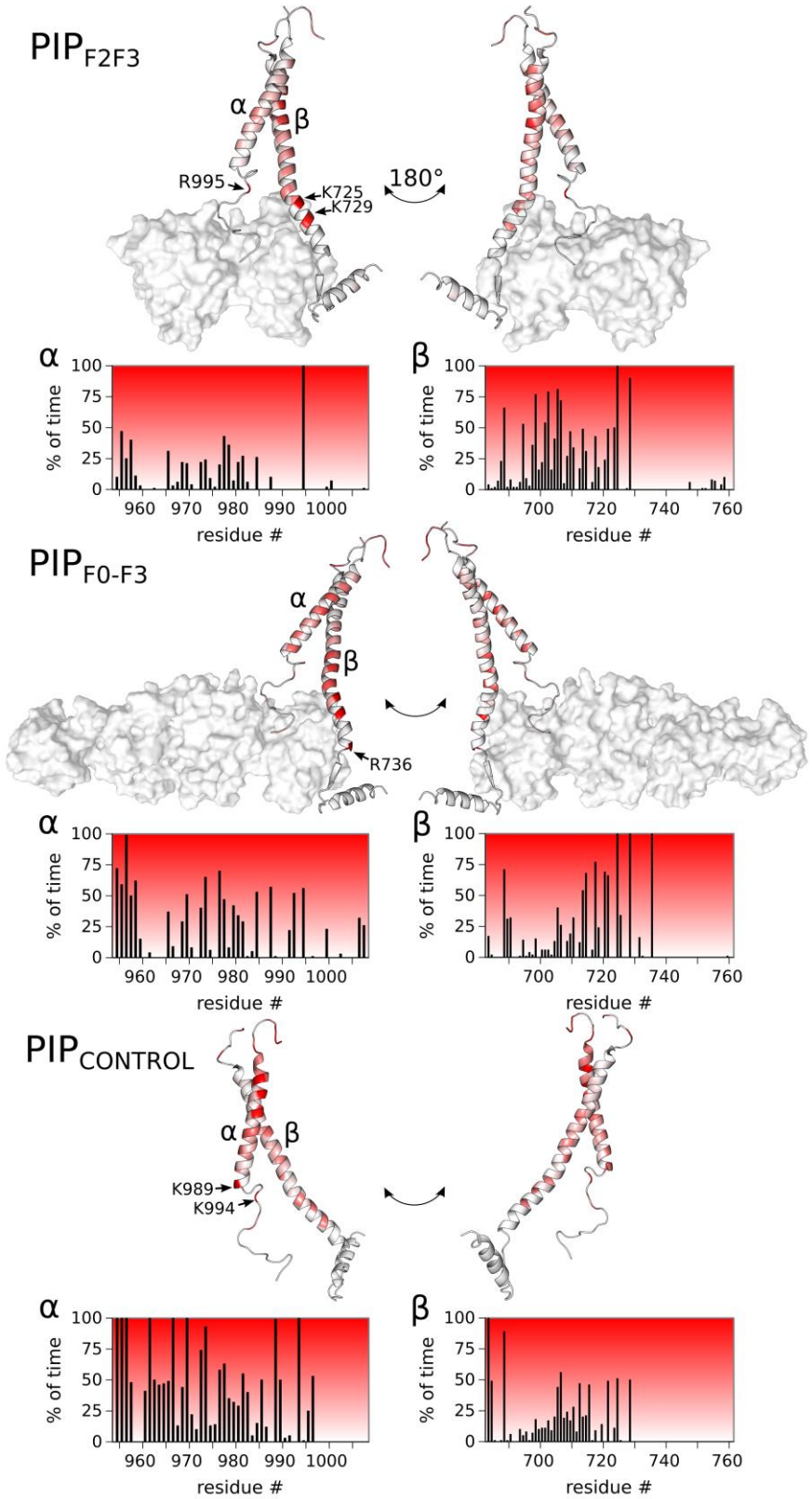

Figure 1. Interactions between integrin and PIP2 lipids. Lipid contact occupancies are mapped on integrin structures in PyMOL (Schrödinger) and presented in separate histograms for the α and β integrins. Occupancy was defined as the percentage of time (during the last 300 ns of the simulation time) when the integrin residue formed contacts with PIP2. Two residues were defined as being in contact when two heavy atoms of different molecules were located at a distance of 0.35 nm or less. The results for PIP_{F2F3} and $PIP_{CONTROL}$ are averages over the two independent simulation repeats (A, B).

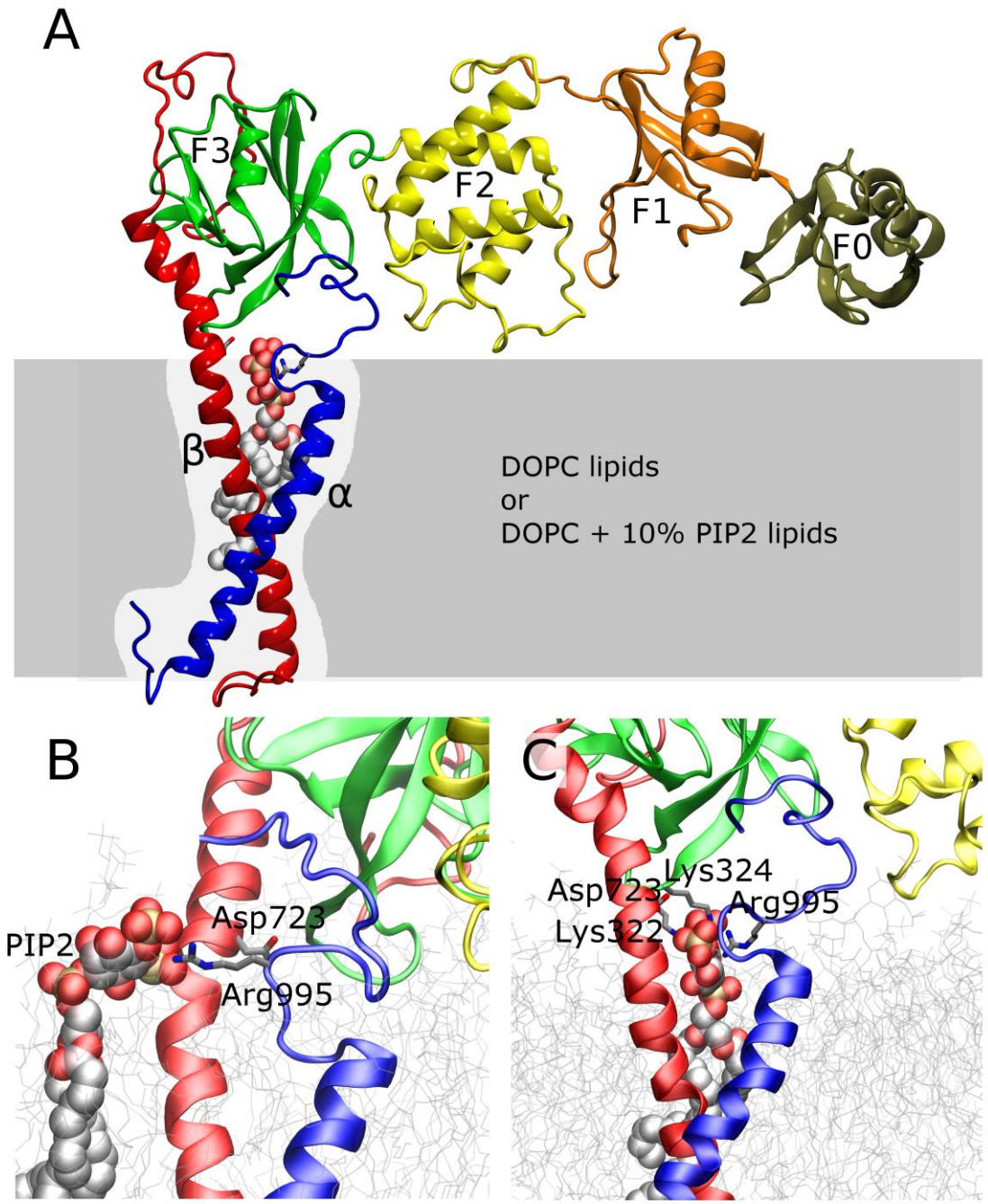

Figure 2. Schematic picture of the simulated system and central findings. A) Schematic picture of the talin head domain in complex with the integrin αIIbβ3 transmembrane and cytoplasmic domains. Integrin αIIb (blue) and β3 (red) chains are embedded in a lipid bilayer (gray). Talin head subdomains F3 (green), F2 (yellow), F1 (orange), and F0 (brown) bind the cytoplasmic tail of integrin β3. PIP2 is shown in the van der Waals (vdW) sphere representation. B) Snapshot of the Arg995-PIP2 contact from the simulation system $PIP_{F2F3\text{-}A}$. The PIP2 lipid interfering with the Asp723-Arg995 interaction is shown in vdW spheres, and other lipids in gray transparent lines. C) Snapshot of the Arg995-Asp723 salt bridge that is broken by the PIP2-Arg995 interaction from the simulation system $PIP_{F0\text{-}F3}$. Snapshots were made using the VMD package.[59]

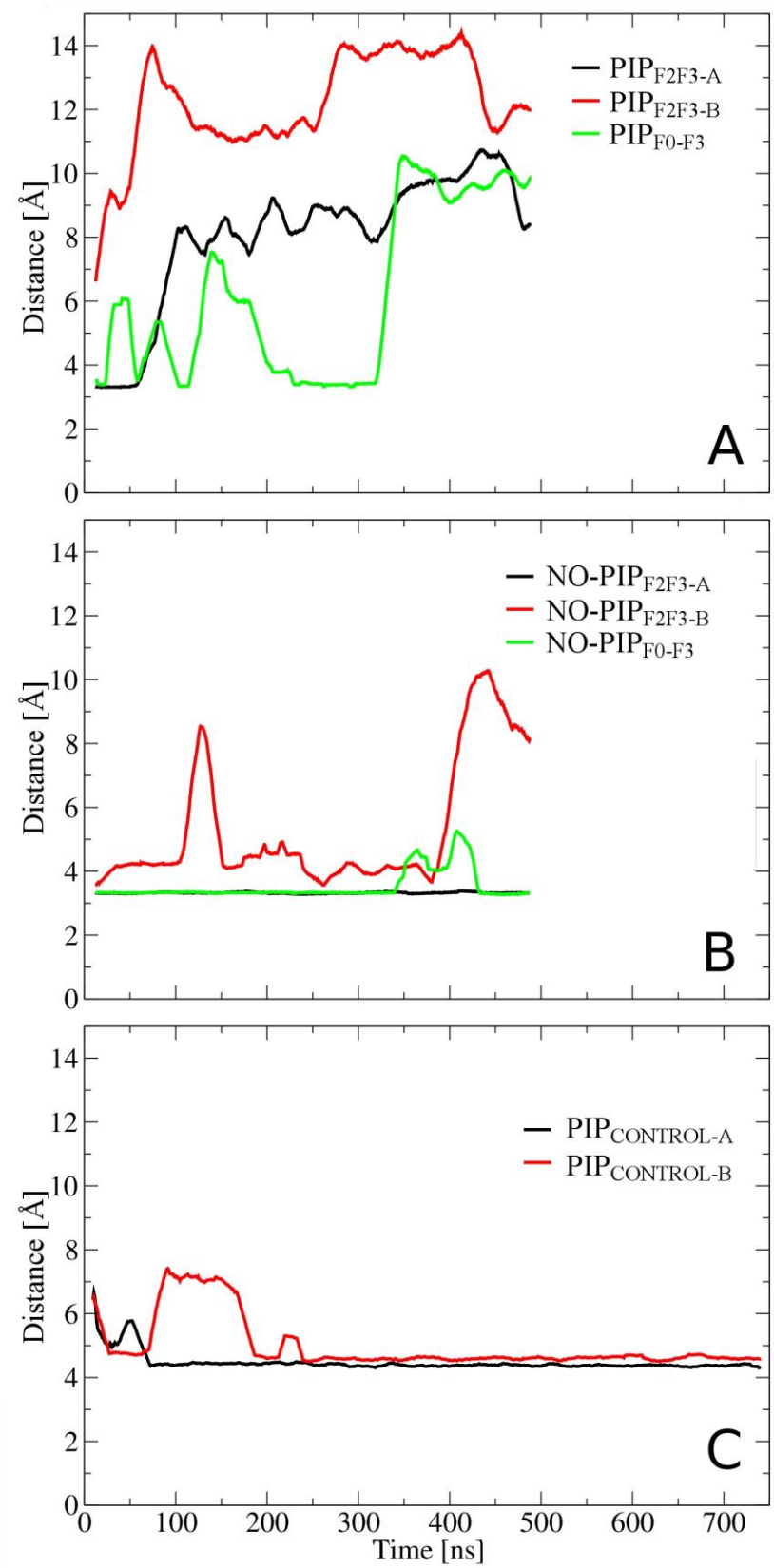

Figure 3. Presence of the Arg995-Asp723 salt bridge. The results show the distance between the Arg995 and Asp723 charged groups. A) Systems with a membrane containing PIP2 and DOPC lipids. B) Systems with a membrane containing only DOPC. C) Systems with a membrane containing PIP2 and DOPC but without talin included in the protein complex. The results shown here were smoothened using a running average over 50 points from a single frame.

3.2 Opening of the Arg995-Asp723 salt bridge— step towards integrin activation?

Having observed the breakage of the Arg995-Asp723 salt bridge, we were tempted to ask whether in the simulations, where PIP2 breaks the Arg995-Asp723 salt bridge, one can see any signs of the initial steps of the integrin activation process. In order to characterize the integrin activation mechanism in more detail, we analyzed a number of parameters suggested to be associated with the activation process.[60,61] Specifically, opening of the integrin dimer at the IMC and OMC and tilting of the transmembrane domain have been proposed to take place in the integrin activation process,[16,18,43,44,45] although recent simulation studies are not conclusive on the mechanism of activation.[60,61,62,63,64] We therefore analyzed the integrin conformation by measuring the helix-helix distance through the distance of Cα atoms of chosen residues at the bottom and at the top of the helices (Figure S3, Table S3), and the tilt angle of the β3-helix in reference to the bilayer normal, representing the helix as a vector between the center of mass of the residues at the bottom and the corresponding center of mass of the residues at the top of the helix (Figure S4, Table S4).

The distance between helices is expected to increase at the IMC and OMC interfaces when the interactions are disrupted.[60] In our analyses, we assume that the distance between the Cα atoms of the residues Val700 and Gly972 measures the stability of OMC, and similarly between Lys716 and Phe993 of IMC. Time evolutions of these distances are shown in Figure S3, and the average values over the last 300 ns of the simulations are depicted in Table S3. The OMC distances remained in the same range whether or not Arg995 and Asp723 were in contact, with the exception of the system $PIP_{CONTROL\text{-}A}$. In $PIP_{CONTROL\text{-}A}$, a DOPC lipid tail entered between Val700 and Gly972 during the first 30 ns of the simulation, possibly suggesting that the OMC contact is not very tight. Separation of the IMC was observed for $PIP_{F0\text{-}F3}$, but its distance remained shorter than in the system $NO\text{-}PIP_{F2F3\text{-}A}$. Therefore, we observe no clear correlation between the existence of the Arg995-Asp723 salt bridge (Figure 3) and the separation of the integrin transmembrane helices.

Another potential indicator of integrin activation is the tilt angle of the integrin β3 helix, which in the non-active state has been shown to be ~25° and is stabilized by the residue Lys716, which keeps the helix in a certain orientation by snorkeling with NH_3^+ towards the phosphate head group region.[65] Time evolution (Figure S4) and average over the last 300 ns of the simulations (Table S4) show that, in three of the cases, the tilt angle is approximately 25°. In the systems $NO\text{-}PIP_{F2F3\text{-}A}$ and $NO\text{-}PIP_{F2F3\text{-}B}$ it is higher (33.37° and 29.43°, respectively), while in the systems $PIP_{F2F3\text{-}A}$, $NO\text{-}PIP_{F0\text{-}F3}$, and $PIP_{CONTROL\text{-}A}$ it is lower (18.12°, 18.00°, and 22.22°, respectively). However, these differences in tilt angle are small,[60, 64] and it is difficult to associate the changes in tilt angle with the existence of the Arg995-Asp723 salt bridge.

Experimental and computational data have been reported to be in favor of the view that talin-induced breakage of the Arg995-Asp723 salt bridge is involved in integrin activation.[14,63] Meanwhile, a recent simulation study questioned the paradigm as to the separation of integrin TM helices upon activation.[64] The authors speculated on the insignificance of the Arg995-Asp723 interaction in talin-mediated integrin activation. Our simulations indicate that this interaction can be disrupted in the presence of ionic lipids such as PIP2, which were not present in any of the previous MD simulation studies of integrin activation by talin.[60,61,62,63,64,66] The models we simulated in this work contain only a small part of the integrin, and there are

many factors causing stress to the αIIbβ3 interface, including conformational changes of the integrin extracellular domain and its interactions with extracellular proteins. Overall, although we can claim the connection between PIP2 and the initialization of inside-out integrin activation process, the data is not sufficient to clarify the impact of the PIP2-induced breakage of the Arg995-Asp723 salt bridge on integrin activation.

3.3 Role of talin in PIP2-mediated integrin activation — joint action of talin and PIP2?

Interactions of talin with lipids have been shown to be an important factor in integrin activation,[19] but some of the related mechanisms are still not clear. To shed light on this matter, in our simulations we included different talin configurations, containing domains F2-F3 (residues 209-400) and F0-F3 (residues 2-398 Δ139-168), to characterize the interactions that occur between talin and a lipid membrane. Similarly to previous analyses of the contacts between integrin tails and PIP2, we carried out contact and hydrogen bond analyses for talin and PIP2/DOPC (Figures 4, S5; Tables S5, S6).

Our data show that there are PIP2 binding spots present in the F0 subdomain: the residues Lys15-Met17, Arg35, and Asp55-Lys58 can bind strongly to PIP2. Subdomains F2 and F3 seem to be very well characterized regarding their affinity towards negatively charged lipids and,[20] indeed, our results show that there are regions within this area that interact very strongly with PIP2, including the residues Glu252-Lys284, Lys318-Arg328, Arg339, Lys343, Ile348, and Lys364. Similar regions tend to bind to DOPC (Figure 4), which is in line with recent studies on the talin-integrin on different lipid bilayer compositions.[61,66] The simulated structure in our study only contained a truncated form of the large loop in the F1 domain; however, this truncated F1 domain loop was found to reside near the membrane, in accordance with previous studies.[42,61] An integrin activation mechanism involving a hydrophobic membrane anchor in the F2 domain of talin was recently predicted in a simulation study.[66] One of the reportedly membrane-inserting phenylalanines was found to reside near the membrane in our simulations (see Phe259 and Phe280 in Figure 4, Table S5 and Table S6), but no anchoring by phenylalanines was observed.

In the simulation of the system $PIP_{F0\text{-}F3}$, the joint action of talin and PIP2 was distinguished. The residues Lys322 and Lys324 in talin F3 domain established hydrogen bond interactions with one of the PIP2 lipids near the integrin helices to further bring it into contact with the residue Arg995 from integrin αIIb. As a result, the important Arg995-Asp723 salt bridge was broken through an interaction between Arg995 and PIP2 lipid headgroup phosphates (see Figure 2C). In the second case where we observed the breakage of the salt bridge mediated by PIP2 (system $PIP_{F2F3\text{-}A}$), talin was not in contact with the PIP2 lipid (for details see Figure 2B). This raises a question whether talin only indirectly facilitates the opening of the IMC by bringing PIP2 lipids into contact with integrin, or whether it has an active role in the process. In the simulations without talin, Arg995 in integrin αIIb did not form contacts to PIP2 lipids, yet its neighboring residue Lys994 was constantly in contact with a PIP2 lipid (Figure 1, Table S1). This suggests that talin is not required for PIP2 lipids to localize near the integrin dimer and the Arg995-Asp723 salt bridge. However, the binding of talin to β3 integrin may expose the Arg995-Asp723 salt bridge to attack by PIP2.

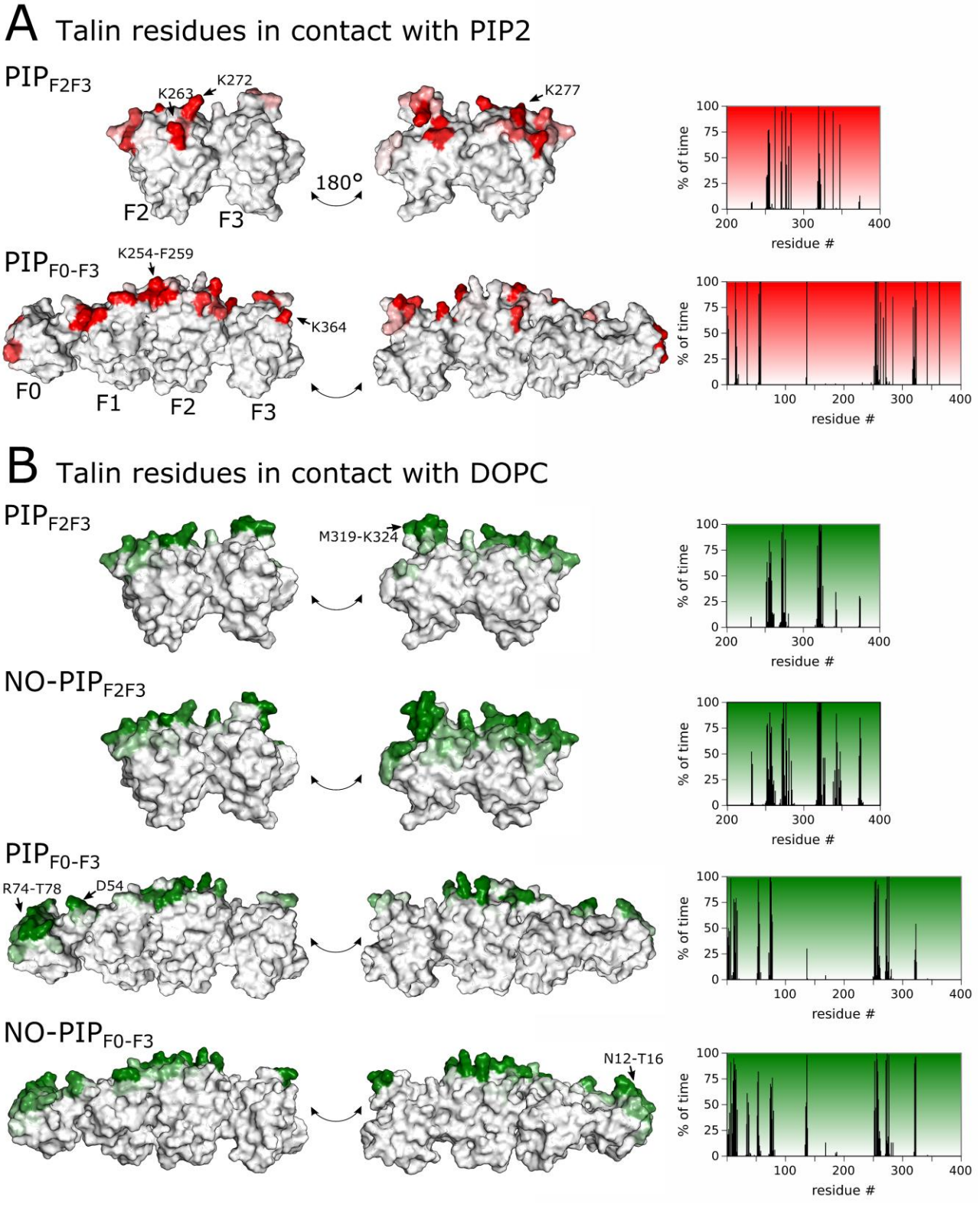

Figure 4. Interactions between talin and A) PIP2 or B) DOPC lipids. Lipid contact occupancies are mapped on talin structures in PyMOL (Schrödinger), and presented in histograms. Occupancy was defined as the percentage of time (during the last 300 ns of the simulation time) when the talin residue formed contacts with a lipid. Two residues were defined as being in contact when two heavy atoms of different molecules were located at a distance of 0.35 nm or less. The results for PIP_{F2F3}, $NO\text{-}PIP_{F2F3}$ and $PIP_{CONTROL}$ and control

simulations are averages over the two independent simulation repeats.

4. Conclusions

Schematic representation of our main results is shown in Figure 5. We propose that PIP2 can have an impact on integrin activation through interaction with talin and Arg995, and break the Arg995-Asp723 salt bridge. Our simulations did not show other clear signs of structural changes in the interaction between the αIIb and β3 chains after the breakdown of the ionic bond.

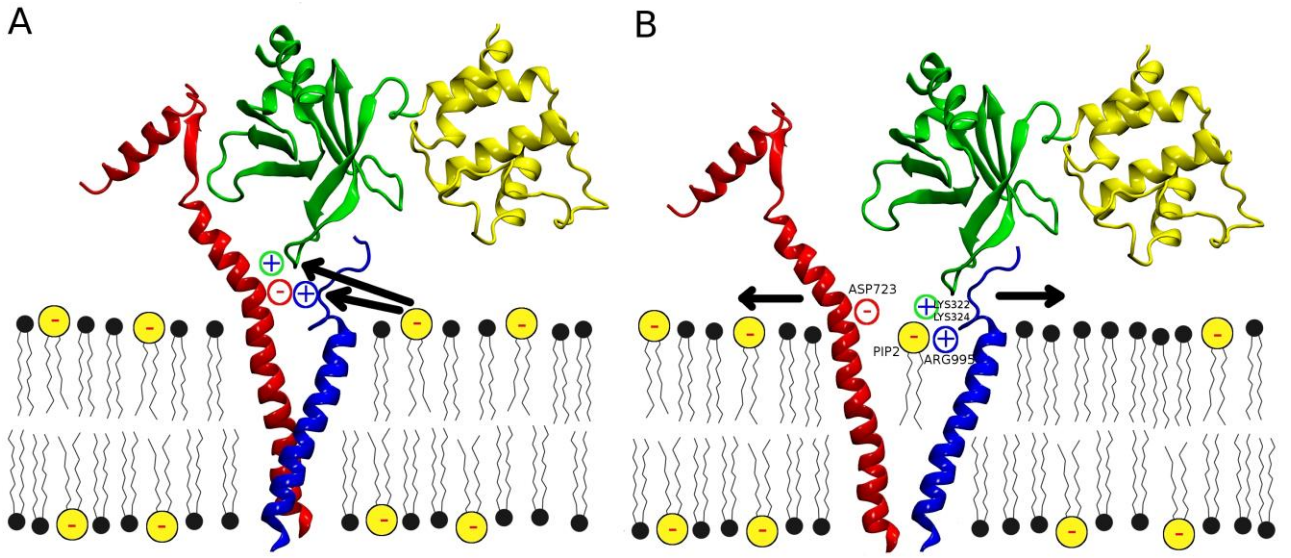

Figure 5. Schematic representation of A) the suggested PIP2-talin-integrin interaction, and B) the suggested activation of the integrin complex mediated by PIP2 and talin. DOPC is depicted with a black and PIP2 with a yellow headgroup. Arrows in the panels A and B indicate the direction of PIP2 movement and possible helix dissociation caused by the breaking of the Arg995-Asp723 salt bridge.

The integrin activation process involves multiple cytoplasmic proteins, and it is possible that the system simulated here is too simplified for the evaluation of further dissociation of the integrin tails and integrin activation. Nevertheless, the fact that experimentally it has been well established that the lack of this salt bridge leads to integrin activation renders our considerations reasonable. Moreover, we recognized other regions of integrin involved in the interactions with PIP2 that might be of high importance in the conformational changes of integrin complexes.

AUTHOR INFORMATION

Corresponding Author

CORRESPONDING AUTHOR FOOTNOTE Tel.: +358 40 198 1010. Fax: +358 3 3115 3015. E-mail: tomasz.rog@gmail.com (T.R.).

Acknowledgements

This work was supported by the Academy of Finland (Center of Excellence program, project no. 272130 (IV); grants 136288 and 273192 (VPH)), the European Research Council (Advanced Grant CROWDED-Pro-LIPIDS (IV)), the Competitive Research Funding of the Tampere University Hospital (VH), and the Sigrid Juselius Foundation (IV). CSC–IT Center for Science (Espoo, Finland) is acknowledged for computational resources. Additionally, the Tampere Graduate Program in Biomedicine and Biotechnology (SK) and the Graduate School program of Tampere University of Technology (SR) are thanked for financial support. This work was granted access to the HPC resources of EPCC made available within the Distributed European Computing Initiative by the PRACE-2IP, receiving funding from the European Community's Seventh Framework Programme (FP7/2007–2013) under grand agreement no. RI-283493.

ASSOCIATED CONTENT

Supplementary Information

Structures of the lipids considered and additional data.

References:

(1) Desgrosellier, J. S.; Cheresh, D. A. Integrins in Cancer: Biological Implications and Therapeutic Opportunities. *Nature Rev. Cancer* **2010**, *10*, 9–22.

(2) Anthis, N. J.; Campbell, I. D. The Tail of Integrin Activation. *Trends Biochem. Sci*. **2011**, *36*, 191–198.

(3) Hynes, R. O. Integrins: Bidirectional, Allosteric Aignaling Machines. *Cell* **2002**, *110*, 673–687.

(4) Shattil, S. J.; Kim, C.; Ginsberg, M. H. The Final Steps of Integrin Activation: The End Game. *Nature Rev. Mol. Cell Biol*. **2010**, *11*, 288–300.

(5) Hughes, P. E.; Diaz-Gonzalez, F.; Leong, L.; Wu, C.; McDonald, J. A.; Shattil, S. J.; Ginsberg, M. H. Breaking the Integrin Hinge. A Defined Structural Constraint Regulates Integrin Signaling. *J. Biol. Chem*. **1996**, *271*, 6571–6574.

(6) Ghevaert, C.; Salsmann, A.; Watkins, N. A.; Schaffner-Reckinger, E.; Rankin, A.; Garner, S. F.; Stephens, J.; Smith, G. A.; Debili, N.; Vainchenker, W.; de Groot, P. G.; Huntington, J. A.; Laffan, M.; Kieffer, N.; Ouwehand, W. H. A Nonsynonymous SNP in the ITGB3 Gene Disrupts the Conserved Membrane-Proximal Cytoplasmic Salt Bridge in the AlphaIIb/beta3 Integrin and Cosegregates Dominantly with Abnormal Proplatelet Formation and Macrothrombocytopenia. *Blood* 2008, *111*, 3407–3414.

(7) Nurden A. T.; Pillois, X.; Wilcox, D. A. Glanzmann Thrombasthenia: State of the Art and Future Directions. *Semin. Thromb. Hemost*. **2013**, *39*, 642–655.

(8) Guan, S.; Tan, S.-M.; Li, Y.; Torres, J.; Uzel, G.; Xiang, L.; Law, S. K. A. Characterization of Single Amino Acid Substitutions in the β2 Integrin Subunit of Patients with Leukocyte Adhesion Deficiency (LAD)-1. *Blood Cells Molecules Dis*. **2015**, *54*, 177–182.

(9) Burridge, K.; Connell, L. A New Protein of Adhesion Plaques and Ruffling Membranes. *J. Cell Biol*. **1983**, *97*, 359–367.

(10) Moser, M.; Legate, K. R.; Zent, R.; Fässler, R. The Tail of Integrins, Talin, and Kindlins. *Science* **2009**, *324*, 895–899.

(11) Critchley, D. R. Biochemical and Structural Properties of the Integrin-Associated Cytoskeletal Protein Talin. *Annual Rev. Biophys*. **2009**, *38*, 235–254.

(12) Calderwood, D. A.; Zent, R.; Grant, R.; Rees, D. J. G.; Hynes, R. O.; Ginsberg, M. H. The Talin Head Domain Binds to Integrin β Subunit Cytoplasmic Tails and Regulates Integrin Activation. *J. Biol. Chem*. **1999**, *274*, 28071–28074.

(13) Tadokoro, S.; Shattil, S. J.; Eto, K.; Tai, V.; Liddington, R. C.; de Pereda, J. M.; Ginsberg, M. H.; Calderwood, D. A. Talin Binding to Integrin ß Tails: a Final Common Step in Integrin Activation. *Science* **2003**, *302*, 103–106.

(14) Ye, F.; Snider, A. K.; Ginsberg, M. H. Talin and Kindlin: the One-Two Punch in Integrin Activation. *Frontiers Med*. **2014**, *8*, 6–16.

(15) García-Alvarez, B.; de Pereda, J. M.; Calderwood, D. A.; Ulmer, T. S.; Critchley, D.; Campbell, I. D.; Ginsberg, M. H.; Liddington, R. C. Structural Determinants of Integrin Recognition by Talin. *Mol. Cell* **2003**, *11*, 49–58.

(16) Wegener, K. L.; Partridge, A. W.; Han, J.; Pickford, A. R.; Liddington, R. C.; Ginsberg, M. H.; Campbell, I. D. Structural Basis of Integrin Activation by Talin. *Cell*, **2007**, *128*, 171–182.

(17) Kim, C.; Ye, F.; Hu, X.; Ginsberg, M. H. Talin Activates Integrins by Altering the Topology of the β Transmembrane Domain. *J. Cell Biol*. **2012**, *197*, 605–611.

(18) Vinogradova, O.; Velyvis, A.; Velyviene, A.; Hu, B.; Haas, T. A.; Plow, E. F.; Qin, J. A. Structural Mechanism of Integrin αIIbβ3 “Inside-Out” Activation as Regulated by Its Cytoplasmic Face. *Cell* **2002**, *110*, 587–597.

(19) Saltel, F.; Mortier, E.; Hytönen, V. P.; Jacquier, M.-C.; Zimmermann, P.; Vogel, V.; Liu, W.;

Wehrle-Haller, B. New PI(4,5)P2- and Membrane Proximal Integrin-Binding Motifs in the Talin Head Control Beta3-Integrin Clustering. *J. Cell Biol.* **2009**, *187*, 715–731.

(20) Moore, D. T.; Nygren, P.; Jo, H.; Boesze-Battaglia, K.; Bennett, J. S.; DeGrado, W. F. Affinity of Talin-1 for the β3-Integrin Cytosolic Domain is Modulated by Its Phospholipid Bilayer Environment. *Proc. Nat. Acad. Sci.* **2012**, *109*, 793–798.

(21) Martel, V.; Racaud-Sultan, C.; Dupe, S.; Marie, C.; Paulhe, F.; Galmiche, A.; Block, M. R.; Albiges-Rizo, C. Conformation, Localization, and Integrin Binding of Talin Depend on Its Interaction with Phosphoinositides. *J. Biol. Chem.* **2001**, *276*, 21217–21227.

(22) Goksoy, E.; Ma, Y.-Q.; Wang, X.; Kong, X.; Perera, D.; Plow, E. F.; Qin, J. Structural Basis for the Autoinhibition of Talin in Regulating Integrin Activation. *Mol. Cell* **2008**, *31*, 124–133.

(23) Song, X.; Yang, J.; Hirbawi, J.; Ye, S.; Perera, H. D.; Goksoy, E.; Dwivedi, P.; Plow, E. F.; Zhang, R.; Qin, J. () A Novel Membrane-Dependent on/off Switch Mechanism of Talin FERM Domain at Sites of Cell Adhesion. *Cell Res.* **2012**, *22*, 1533–1545.

(24) McLaughlin, S.; Wang, J.; Gambhir, A.; Murray, D. PIP(2) and Proteins: Interactions, Organization, and Information Flow. *Ann. Rev. Biophys. Biomol. Struct.* **2002**, *31*, 151–175.

(25) Xu, C.; Watras, J.; Loew, L. M. Kinetic Analysis of Receptor-Activated Phosphoinositide Turnover. *J. Cell Biol.* **2003**, *161*, 779–791.

(26) Ling, K.; Doughman, R. L.; Firestone, A. J.; Bunce, M. W.; Anderson, R. A. Type Iγ Phosphatidylinositol Phosphate Kinase Targets and Regulates Focal Adhesions. *Nature* **2002**, *420*, 89–93.

(27) Di Paolo, G.; Pellegrini, L.; Letinic, K.; Cestra, G.; Zoncu, R.; Voronov, S.; Chang, S.; Guo, J.; Wenk, M. R.; De Camilli, P. Recruitment and Regulation of Phosphatidylinositol Phosphate Kinase Type 1 Gamma by the FERM Domain of Talin. *Nature* **2002**, *420*, 85–89.

(28) Sun, Y.; Thapa, N.; Hedman, A. C.; Anderson, R.A. Phosphatidylinositol 4,5-Bisphosphate: Targeted Production and Signaling. *Bioessays* **2013**, *35*, 513–522.

(29) Kwiatkowska, K. One Lipid, Multiple Functions: How Various Pools of PI(4,5)P2 Are Created in the Plasma Membrane. *Cell. Mol. Life Sci*. **2010**, *67*, 3927–3946.

(30) van den Bout, I.; Divecha, N. PIP5K-Driven PtdIns(4,5)P2 Synthesis: Regulation and Cellular Functions. *J. Cell Sci*. **2009**, *122*, 3837–3850.

(31) Chinthalapudi, K.; Rangarajan, E. S.; Patil, D. N.; George, E. M.; Brown, D. T.; Izard, T. Lipid Binding Promotes Oligomerization and Focal Adhesion Activity of Vinculin. *J. Cell Biol*. **2014**, *207*, 643–656.

(32) Raghunathan, V.; Mowery, P.; Rozycki, M.; Lindberg, U.; Schutt, C. Structural Changes in Profilin Accompany its Binding to Phosphatidylinositol, 4,5-Bisphosphate. *FEBS Letters* **1992**, *297*, 46–50.

(33) Hirao, M.; Sato, N.; Kondo, T.; Yonemura, S.; Monden, M.; Sasaki, T.; Takai, Y.; Tsukita, S.; Tsukita, S. Regulation Mechanism of ERM (Ezrin/Radixin/Moesin) Protein/Plasma Membrane Association: Possible Involvement of Phosphatidylinositol Turnover and Rho-Dependent Signaling Pathway. *J. Cell Biol*. **1996**, *135*, 37–51.

(34) Li, L.; Shi, X.; Guo, X.; Li, H.; Xu, C. Ionic Protein-Lipid Interaction at the Plasma Membrane: What Can the Charge Do? *Trends Biochem. Sci*. **2014**, *39*, 130–140.

(35) Kuo, W.; Herrick, D. Z.; Cafiso, D. S. Phosphatidylinositol 4,5 Bisphosphate Alters Synaptotagmin 2 Membrane Docking and Drives Opposing Bilayers Closer Together. *Biochemistry* **2011**, *50*, 2633–2641.

(36) Steringer, J. P.; Bleicken, S.; Andreas, H.; Zacherl, S.; Laussmann, M.; Temmerman, K.; Contreras, F. X.; Bharat, T. A.; Lechner, J.; Müller, H. M.; Briggs, J. A.; García-Sáez, A. J.; Nickel, W. Phosphatidylinositol 4,5-Bisphosphate (PI(4,5)P2)-Dependent Oligomerization Offibroblast

Growth Factor 2 (FGF2) Triggers the Formation of a Lipidic Membrane Pore Implicated in Unconventional Secretion. *J. Biol. Chem.* **2012**, *287*, 27659–27669.

(37) Coskun, Ü.; Grzybek, M.; Drechsel, D.; Simons, K. Regulation of Human EGF Receptor by Lipids. *Proc. Nat. Acad. Sci. USA* **2011**, *108*, 9044–9048.

(38) Coskun, U.; Simons, K. Cell Membranes: the Lipid Perspective. *Structure* **2011**, *19*, 1543–1548.

(39) Pöyry, S.; Cramariuc, O.; Postila, P.A.; Kaszuba, K.; Sarewicz, M.; Osyczka, A.; Vattulainen, I.; Róg, T. Atomistic Simulations Indicate Cardiolipin to Have an Integral Role in the Structure of the Cytochrome bc1 Complex. *Biochim. Biophys. Acta* **2013**, *1827*, 769–778.

(40) Sali, A.; Blundell, T. L. Comparative Protein Modelling by Satisfaction of Spatial Restraints. *J. Mol. Biol.* **1993**, *234*, 779–815.

(41) Elliott, P. R.; Goult, B. T.; Kopp, P. M.; Bate, N.; Grossmann, J. G.; Roberts, G. C. K.; Critchley, D. R.; Barsukov, I. L. The Structure of the Talin Head Reveals a Novel Extended Conformation of the FERM Domain. *Structure* **2010**, *18*, 1289–1299.

(42) Goult, B. T.; Bouaouina, M.; Elliott, P. R.; Bate, N.; Patel, B.; Gingras, A. R.; Grossmann, J. G.; Roberts, G. C. K.; Calderwood, D. A.; Critchley, D. R.; Barsukov, I. L. Structure of a Double Ubiquitin-Like Domain in the Talin Head: a Tole in Integrin Activation. *EMBO J.* **2010**, *29*, 1069–1080.

(43) Anthis, N. J.; Wegener, K. L.; Ye, F.; Kim, C.; Goult, B. T.; Lowe, E. D.; Vakonakis, I.; Bate, N.; Critchley, D. R.; Ginsberg, M. H.; Campbell, I. D. The Structure of an Integrin/Talin Complex Reveals the Basis of Inside-Out Signal Transduction. *EMBO J.* **2009**, *28*, 3623–3632.

(44) Lau, T.-L.; Kim, C.; Ginsberg, M. H.; Ulmer, T. S. The Structure of the Integrin αIIbβ3 Transmembrane Complex Explains Integrin Transmembrane Signalling. *EMBO J.* **2009**, *28*, 1351–1361.

(45) Yang, J.; Ma, Y.-Q.; Page, R.C.; Misra, S.; Plow, E. F.; Qin, J. Structure of an Integrin αIIbβ3 Transmembrane-Cytoplasmic Heterocomplex Provides Insight Into Integrin Activation. *Proc. Nat. Acad. Sci. USA* **2009**, *106*, 17729–17734.

(46) Metcalf, D. G.; Moore, D. T.; Wu, Y.; Kielec, J. M.; Molnar, K.; Valentine, K. G.; Wand, A. J.; Bennett, J. S.; DeGrado, W. F. NMR Analysis of the αIIbβ3 Cytoplasmic Interaction Suggests a Mechanism for Integrin Regulation. *Proc. Nat. Acad. Sci*. **2010**, *107*, 22481–22486.

(47) Jorgensen, W. L.; Tirado-Rives, J. The OPLS [Optimized Potentials for Liquid Simulations] Potential Functions for Proteins, Energy Minimizations for Crystals of Cyclic Peptides and Crambin. *J. Ame. Chem. Soc*. **1988**, *110*, 1657–1666.

(48) Maciejewski, A.; Pasenkiewicz-Gierula, M.; Cramariuc, O.; Vattulainen, I.; Rog, T. Refined OPLS All-Atom Force Field for Saturated Phosphatidylcholine Bilayers at Full Hydration. *J. Phys. Chem. B* **2014**, *118*, 4571–4581.

(49) Jorgensen, W. L.; Chandrasekhar, J.; Madura, J. D.; Impey, R. W.; Klein, M. L. Comparison of Simple Potential Functions for Simulating Liquid Water. *J. Chem. Phys*. **1983**, *79*, 926–935.

(50) Kaiser, H.-J.; Orłowski, A.; Róg, T.; Nyholm, T. K. M.; Chai, W.; Feizi, T.; Lingwood, D.; Vattulainen, I.; Simons, K. Lateral Sorting in Model Membranes by Cholesterol-Mediated Hydrophobic Matching. *Proc. Nat. Acad. Sci. USA* **2011**, *108*, 16628–16633.

(51) Orłowski, A.; St-Pierre, J.-F.; Magarkar, A.; Bunker, A.; Pasenkiewicz-Gierula, M.; Vattulainen, I.; Róg, T. Properties of the Membrane Binding Component of Catechol-O-Methyltransferase Revealed by Atomistic Molecular Dynamics Simulations. *J. Phys. Chem. B* **2011**, *115*, 13541–13550.

(52) Hess, B.; Bekker, H.; Berendsen, H. J. C.; Fraaije, J. G. E. M. LINCS: a Linear Constraint Solver for Molecular Simulations. *J. Comput. Chem*. **1997**, *18*, 1463–1472.

(53) Parrinello, M.; Rahman, A. Polymorphic Transitions in Single Crystals: a New Molecular Dynamics Method. *J. Appl. Phys*. **1981**, *52*, 7182–7190.

(54) Bussi, G.; Donadio, D.; Parrinello, M. Canonical Sampling through Velocity Rescaling. *J. Chem. Phys.* **2007**, *126*, 014101.

(55) Essmann, U.; Perera, L.; Berkowitz, M. L.; Darden, T.; Lee, H.; Pedersen, L. G. A Smooth Particle Mesh Ewald Method. *J. Chem. Phys*. **1995**, *103*, 8577–8593.

(56) Hess, B.; Kutzner, C.; van der Spoel, D.; Lindahl, E. GROMACS 4: Algorithms for Highly Efficient, Load-Balanced, and Scalable Molecular Simulation. *J. Chem. Theory Comput*. **2008**, *4*, 435–447.

(57) Kim, C.; Lau, T-L.; Ulmer, T. S.; Ginsberg, M. H. Interactions of Platelet Integrin αIIb and β3 Transmembrane Domains in Mammalian Cell Membranes and Their Role in Integrin Activation. *Blood* **2009**, *113*, 4747–4753

(58) Murzyn, K.; Róg, T.; Jezierski, G.; Kitamura, K.; Pasenkiewicz-Gierula, M. Effects of Phospholipid Unsaturation on the Membrane/Water Interface: A Molecular Simulation Study. *Biophys. J*. **2001**, *81*, 170–183.

(59) Humphrey, W.; Dalke, A.; Schulten, K. VMD: visual molecular dynamics. *J. Mol. Graphics* **1996**, *14*, 33–38.

(60) Kalli, A. C.; Campbell, I. D.; Sansom, M. S. P. Multiscale Simulations Suggest a Mechanism for Integrin Inside-Out Activation. *Proc. Nat. Acad. Sci. USA* **2011**, *108*, 11890–11895.

(61) Kalli, A. C.; Campbell, I. D.; Sansom, M. S. P. Conformational Changes in Talin on Binding to Anionic Phospholipid Membranes Facilitate Signaling by Integrin Transmembrane Helices. *PLoS Comput. Biol*. **2013**, *9*, e1003316.

(62) Kalli, A. C.; Wegener, K. L.; Goult, B. T.; Anthis, N. J.; Campbell, I. D.; Sansom, M. S. P. The Structure of the Talin/Integrin Complex at a Lipid Bilayer: an NMR and MD Simulation Study. *Structure* **2010**, *18*, 1280–1288.

(63) Mehrbod, M.; Trisno, S.; Mofrad, M. R. K. On the Activation of Integrin αIIbβ3: Outside-In and Inside-Out Pathways. *Biophys. J.* **2013**, *105*, 1304−1315.

(64) Provasi, D.; Negri, A.; Coller, B. S.; Filizola, M. Talin-Driven Inside-Out Activation Mechanism of Platelet αIIbβ3 Integrin Probed by Multi-Microsecond, All-Atom Molecular Dynamics Simulations. *Proteins* **2014**, *82*, 3231–3240.

(65) Kim, C.; Schmidt, T.; Cho, E.-G.; Ye, F.; Ulmer, T. S.; Ginsberg, M. H. Basic amino-acid side chains regulate transmembrane integrin signalling. *Nature* **2012**, *481*, 209–213.

(66) Arcario, M. J.; Tajkhorshid, E. Membrane-Induced Structural Rearrangement and Identification of a Novel Membrane Anchor in Talin F2F3. *Biophys. J.* **2014**, *107*, 2059–2069.

Table of Contents (TOC) Image